BIOCHEMISTRY
including biophysical chemistry & molecular biology
Article

Biochemistry **2010,** *49,* 29–35 29
DOI: 10.1021/bi901572f

Identification of a Functionally Important Loop in *Salmonella typhimurium* ArnT†

Nicholas A. Impellitteri, Jacqueline A. Merten, Lynn E. Bretscher, and Candice S. Klug*

Department of Biophysics, Medical College of Wisconsin, 8701 Watertown Plank Road, Milwaukee, Wisconsin 53226

Received September 8, 2009; Revised Manuscript Received November 25, 2009

ABSTRACT: ArnT confers resistance to the antibiotic polymyxin in *Salmonella typhimurium* and *Escherichia coli* through the modification of lipid A, a major component of the outer surface of Gram-negative bacteria. ArnT transfers a neutral aminoarabinose moiety onto the negative phosphate groups of lipid A, reducing the surface charge of the bacteria and preventing cationic peptides such as polymyxin from electrostatically recognizing and killing the bacteria. We previously reported the first expression, purification, and functional analysis of ArnT from *S. typhimurium* [Bretscher, L. E., Morrell, M. T., Funk, A. L., and Klug, C. S. (2006) *Protein Expression Purif. 46*, 33−39]. Our studies showed that ArnT is highly α-helical and described a new *in vivo* functional growth assay. Here, we use the cysteine-specific mPEG-mal to demonstrate that all eight of the native cysteines in *S. typhimurium* ArnT are in the reduced form and not involved in disulfide bonds and show that the cysteine-free protein is structurally and functionally intact as characterized by circular dichroism and the *in vivo* growth assay. Following this initial characterization, *in vivo* expression and function profiles were surveyed for 31 consecutive mutations within a putative ArnT loop. These studies identify for the first time 14 residues that are essential for function of the ArnT transferase and 3 additional residues that completely disrupt protein folding or insertion into the bacterial inner membrane.

The proteins and substrates involved in the ability of bacteria such as *Salmonella typhimurium* and *Escherichia coli* to develop resistance to antimicrobial peptides are continuing to be identified based on genetic analysis. One of the proteins discovered to be specifically involved in resistance to the antibiotic polymyxin is the inner membrane protein ArnT, which confers resistance to polymyxin through the modification of lipid A, the major component of the outer leaflet of the outer membranes of Gram-negative bacteria (*2*). ArnT is responsible for the transfer of a neutral L-Ara4N[1] (4-amino-4-deoxy-L-arabinose) moiety onto one or both of the negative phosphate groups of lipid A prior to localization to the outer leaflet (*3*). The L-Ara4N is attached to an undecaprenyl phosphate lipid precursor, which is synthesized by an array of cytoplasmic proteins and inserted into the inner membrane. The modification of lipid A reduces the overall negative charge of the cell surface, preventing cationic peptides such as polymyxin from recognizing and binding electrostatically to the bacterial surface, thus causing the bacteria to become resistant to polymyxin (*4*). ArnT from *S. typhimurium* contains 548 amino acids and has 80% sequence similarity (69% identity) to ArnT derived from *E. coli*. The small number of other sequences with any significant homology to the ArnT protein are "hypothetical proteins" with no structural information, indicating that little is known about this type of transferase. We have previously reported the purification of *S. typhimurium* ArnT using a 6×-His tag and nickel chromatography and have shown that the secondary structure of the WT (wild-type) ArnT protein is approximately 75% α-helical, as would be expected for an inner membrane protein (*1*). We now present circular dichroism (CD) data in the presence of a reducing agent that shows that the secondary structure of ArnT is not dependent on disulfide bridges. In addition, we demonstrate that *S. typhimurium* ArnT contains no disulfide bonds, despite the presence of eight native cysteines, and we have created and characterized a functional cysteine-free protein. Expression studies show that only small amounts of ArnT are necessary to provide resistance against polymyxin to the bacterial cell, and analysis of 31 point mutations within a putative periplasmic loop of the cysteine-free ArnT protein has been carried out using an *in vivo* growth assay (*1*) coupled with expression studies, allowing us to identify for the first time specific critical residues within this bacterial transferase. These critical residues fall into two categories: those that disrupt initial protein folding or membrane localization and those that fail to confer *in vivo* resistance to polymyxin despite being expressed to the inner membrane.

EXPERIMENTAL PROCEDURES

Topology Model. The membrane helical segments were predicted using TMMOD analysis of the protein sequence (*5*). Analysis predicted 11 helical segments, with a large (125 residues) soluble C-terminal segment and a 60% probability that the N-terminus faces the cytoplasm. A Kyte−Doolittle hydropathy plot (SeqWeb (*6*)) indicated that the protein is generally hydrophobic, with several hydrophilic spikes that include residues Q30, K110, K200, and H505, all of which are located in loops in the model. Analysis by TMHMM 2.0 (www.cbs.dtu.dk/services/TMHHM/), DAS-TMfilter (*7*), and SOSUI (*8*) showed similar general trends for the helical regions, though disagreed on the exact identification of membrane-spanning residues, number of helices (11−13), and cellular location of the N- and C-termini.

†This work was supported by the NIH (AI058024).
*Corresponding author. Phone: 414-456-4015. Fax: 414-456-6512. E-mail: candice@mcw.edu.
[1]Abbreviations: L-Ara4N, 4-amino-4-deoxy-L-arabinose; mPEG-mal (mPEG-MAL-5000), maleimide-coupled polyethylene glycol of molecular mass 5000 Da; CD, circular dichroism; 2A6S, C148A/C149A/C173S/C216S/C318S/C383S/C400S/C411S (2 Ala and 6 Ser substituted cysteine-free ArnT protein); DM, dodecyl maltoside.

Published on Web 11/30/2009

Site-Directed Mutagenesis and Protein Purification. Cysteine substitutions were carried out using mutant primers (Integrated DNA Technologies, Coralville, IA) and the QuikChange mutagenesis kit (Stratagene, La Jolla, CA) following the manufacturer's directions. Mutant plasmids were verified by sequencing at the Protein and Nucleic Acid Shared Facility (Medical College of Wisconsin).

The plasmid-encoded *arnT* gene with a 6×-His tag and containing a single P547A mutation (termed WT) was transformed into *E. coli* NovaBlue (Novagen, EMD Biosciences, Germany) cells and grown at 37 °C in Luria−Bertani (LB) broth containing 100 μg/mL ampicillin (*9*). Expression was induced by the addition of 1 mM IPTG (isopropyl 1-thio-β-D-galactopyranoside), and membrane proteins were extracted using 1% DM (dodecyl maltoside). For CD analysis, the WT and cysteine-free ArnT proteins were further purified by cobalt affinity (Talon resin; Clontech BD Biosciences, San Jose, CA) chromatography and elution with 100 mM imidazole.

Expression Analysis. For expression studies, the solubilized membrane protein fractions from two or three separate cultures with similar optical densities were subjected to SDS−PAGE, and ArnT was identified by Western blot analysis using a TetraHis antibody (Qiagen, Valencia, CA) and quantitated by densitometry (ImageJ; NIH, Bethesda, MD) with the same cysteine-free (2A6S) control run on each gel. Total membrane protein was determined by the BCA protein assay kit (BCA Protein Assay; Thermo Fisher Pierce), and ArnT was quantitated by Western blot using 30−130 ng of affinity-purified cysteine-free ArnT protein as a concentration standard.

PEG Assay. Five microliters of 35 mM mPEG-MAL-5000 (Nektar Therapeutics, San Carlos, CA) in 50 mM Tris, pH 8, 10% glycerol, 0.01% DM, and 100 mM imidazole was added to 15 μL of wild-type or cysteine-free (2A6S) ArnT (12 μg total protein) in the same buffer and incubated at room temperature for 2.5 h. The control sample contained 5 μL of protein without the addition of 800× (100× per native cysteine) mPEG-MAL-5000 and was also incubated at room temperature for 2.5 h. Samples were then subjected to 7.5% SDS−PAGE for 3.5 h, and the protein bands were observed by silver staining.

Circular Dichroism. The secondary structure of ArnT was assessed by circular dichroism (CD) spectroscopy on a Jasco 710 spectropolarimeter using a 1.0 mm cell length. ArnT concentrations were 0.20−0.27 mg/mL in 50 mM sodium phosphate, pH 7, and 0.01% DM buffer. Spectra were recorded from 190 to 250 nm, and the background spectrum was recorded on a sample containing buffer without protein. Spectral analysis was carried out by submitting the spectroscopic data to DICHROWEB, the online circular dichroism Web site (http://www.cryst.bbk.ac.uk/cdweb/html/home.html), which is supported by grants to the BBSRC Center for Protein and Membrane Structure and Dynamics (*10*). ContinLL (*11*, *12*) and K2d (*13*) algorithms gave the best fits to the data and were used for secondary structure quantitation.

Growth Assay. The *in vivo* growth assay of the mutant ArnT proteins was modified from our previously described method (*1*) by taking advantage of our *E. coli* BL21(DE3) chromosomal knockout of the *arnT* gene, BL21(DE3)ΔArnT. Cultures containing 10^5 cells in 2 mL of LB/ampicillin were incubated and shaken in the presence and absence of 2 μg/mL polymyxin in 24-well microplates overnight at 37 °C. Growth was quantitated spectrophotometrically at 600 nm in a microplate reader (Thermo Scientific). Assays were carried out twice in duplicate and compared to both an empty vector (pET21) and P547A ArnT (WT) as polymyxin-sensitive and polymyxin-resistant controls, respectively.

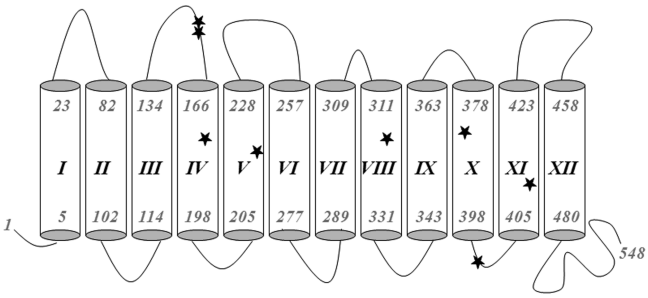

FIGURE 1: Topology model of the proposed helical arrangement in ArnT. Stars indicate the predicted amino acid positions of each of the eight native cysteines.

RESULTS

Topology Model. The structural topography of the predicted transmembrane helices of ArnT is shown in Figure 1. This is the first model of the 548 amino acid *S. typhimurium* ArnT protein and serves as a starting point for the functional studies presented here. The model is based in part on TMMOD analysis (*14*), which predicted 11 transmembrane segments and a large C-terminal soluble domain (helix XII in the model was not predicted by TMMOD), and by analogy to other inner membrane proteins (e.g., AcrB (*15*), MsbA (*16*), P-glycoprotein (*17*), CFTR (*18*)) that contain 12 helices. In addition, ArnT was shown by CD to have a very high content of α-helical structure (*1*), as is the case with most inner membrane proteins. Since there is no sequence homology to other proteins, the ArnT structure is either a completely new fold or, more likely, belongs to a class of inner membrane proteins having high structural similarity with little or no sequence homology. Therefore, 12 transmembrane helical segments are proposed as a starting point in this model.

It is possible that this protein is not solely made up of long transmembrane α-helices and unstructured loops but also includes secondary structure in the loop regions with helices or β-strands that cannot be predicted at this time, especially in the large span of amino acids predicted to make up the C-terminal domain. The predicted topology locates only three of the native cysteines within loops, although it is not unprecedented to have free cysteines in transmembrane α-helices (e.g., refs *19* and *20*). The locations of the cysteines in loops on either side of the membrane and within the membrane are consistent with our data presented below confirming that none of the native cysteines form disulfide bonds.

Quantitation of Free Cysteines. ArnT is a 62 kDa protein that runs at approximately 59 kDa by SDS−PAGE analysis, as we determined previously (*1*). Reaction of free cysteine residues with a cysteine-specific maleimide linked to PEG_{5000} (mPEG-mal) allows quantitation of the free cysteines by SDS−PAGE due to the large molecular mass (6000 Da) of mPEG-mal (*21*, *22*). Each addition of mPEG-mal to a protein results in an approximately 6 kDa increase in apparent molecular mass as judged by SDS−PAGE. In order to determine how many of the eight native cysteines in *S. typhimurium* ArnT are freely reactive and how many are involved in disulfide bonds, a PEGylation experiment was carried out on the purified wild-type (WT) protein. WT ArnT was reacted with an excess of mPEG-mal for 2.5 h at room temperature before being analyzed by SDS−PAGE (Figure 2A).

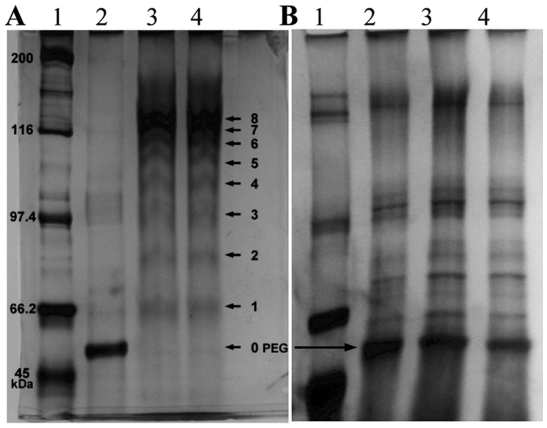

FIGURE 2: 7.5% SDS−PAGE gel showing the results of the mPEG-mal modification for the (A) WT and (B) 2A6S (cysteine-free) experiments. Lane 1 contains molecular mass standards, lane 2 contains purified ArnT protein, and lanes 3 and 4 contain duplicate samples of ArnT after reaction with excess mPEG-mal. Each addition of one mPEG-mal moiety is marked by an arrow.

The control sample in lane 2 containing no mPEG-mal is marked by the 0 PEG arrow and is consistent with monomeric, unmodified ArnT. The duplicate samples run in lanes 3 and 4 that were reacted with mPEG-mal reveal a ladder of protein bands, clearly indicating eight sets of modified ArnT. All of the protein present was modified to some extent, as indicated by the absence of a protein band at the 0-PEG position. A small amount of the protein sample was modified with only one, two, three, four, or five mPEG-mal moieties, while the majority of the protein contained the addition of six, seven, or eight mPEG-mal moieties. This suggests that, even in the absence of a reducing agent, all eight of the ArnT cysteines are freely reactive and not involved in disulfide bonds.

Creation of a Cysteine-Free ArnT. Since none of the cysteines in ArnT are involved in disulfide linkages and all eight are freely reactive, substitutions were made in the protein to create a cysteine-free ArnT. Activities of the ArnT protein variants were assayed using our previously developed polymyxin-sensitive ArnT knockout strain BL21(DE3)ΔArnT (*1*). Mutant plasmids were each transformed into BL21(DE3)ΔArnT cells, where the chromosomal *arnt* gene has been deleted, and assayed for plasmid-encoded ArnT functionality by assessing the ability of the bacteria to grow in the presence of polymyxin. Initially, we mutated all of the eight native cysteines, C148, C149, C173, C216, C318, C383, C400, and C411 (Figure 3), to serines (abbreviated as 8S) by site-directed mutagenesis to create a cysteine-free construct. However, the growth assay data showed that the 8S cysteine-free ArnT protein was inactive (Table 1), as indicated by the inability of the transformed bacteria to grow in the presence of polymyxin. In contrast, bacteria transformed with the WT plasmid grew in polymyxin-containing media, demonstrating that the WT protein was functional, as expected. Toward the goal of producing a functional, cysteine-free ArnT protein, a modified cysteine-free mutant construct was made by mutating both C148 and C149 to alanine while the remaining cysteines remained substituted with serine (abbreviated 2A6S). When assayed for growth in the presence of polymyxin, the 2A6S cysteine-free construct of ArnT supported growth at a level similar to that of the native protein (Table 1). An additional mutant with the native cysteine residues at sites 148 and 149 (2C6S) also conferred resistance to polymyxin.

```
  1  MMKSIRYYLAFAAFIALYYVIPVNS
     RLLWQPDETRYAEISREMLASGDWI  50
 51  VPHFLGLRYFEKPIAGYWINSLGQW
     LFGATNFGVRAGAILTTLLAAALVA 100
101  WLTFRLWRDKRTALLASVIFLSLFA
     VYSIGTYAVLDPMIALWLTAGMCCF 150
151  WQGMQATTRMGKIGMFLLLGATCGL
     GVLTKGFLALAVPVVSVLPWVIVQK 200
201  RWKDFLLYGWLAVLSCFVVVLPWAI
     AIARREADFWHYFFWVEHIQRFAMS 250
251  DAQHKAPFWYYLPVLLAGSLPWLGL
     LPGALKLGWRERNGAFYLLGWTIMP 300
301  LLFFSIAKGKLPTYVLSCFAPIAIL
     MARFVLHNVKEGVAALRVNGGINLV 350
351  FGLVGIVAAFVVSSWGPLKSPVWTH
     IETYKVFCVWGVFTVWAFVGWYSLC 400
401  HSQKYLLPAFCPLGLALLFGFSIPD
     RVMESKQPQFFVEMTQAPLASSRYI 450
451  LADNVGVAAGLAWSLKRDDIMLYGH
     AGELRYGLSYPDVQDKFVKADDFNA 500
501  WLNQHRQEGIITLVLSIAKDEDISA
     LSLPPADNIDYQGRLVLIQYRPK   548
```

FIGURE 3: Primary sequence of the *S. typhimurium* ArnT protein with the eight native cysteines highlighted.

Table 1: Mutant Construct Compositions and Corresponding Polymyxin-Sensitivity Growth Assay Results

148	149	173	216	318	383	400	411	OD_{600}
Cys	*Cys*	*Cys*	*Cys*	*Cys*	*Cys*	*Cys*	*Cys*	0.96 ± 0.10
Ser	Ser	Ser	Ser	Ser	Ser	Ser	Ser	0.02 ± 0.02
Ala	Ala	Ser	Ser	Ser	Ser	Ser	Ser	0.84 ± 0.09
Cys	*Cys*	Ser	Ser	Ser	Ser	Ser	Ser	0.68 ± 0.05

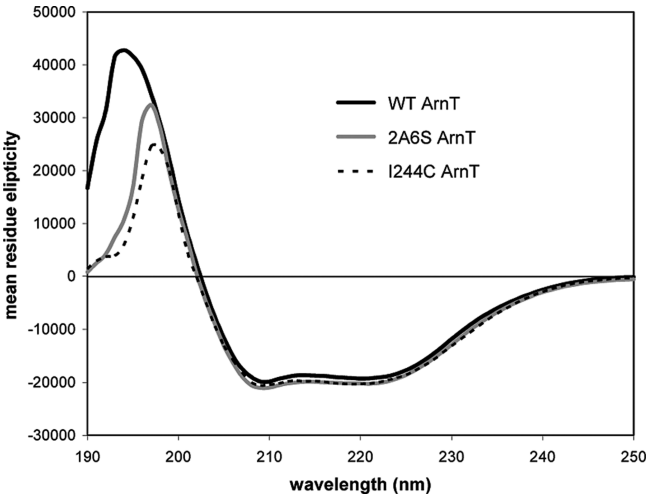

FIGURE 4: Circular dichroism spectra of purified WT, cysteine-free (2A6S), and I244C (in the 2A6S background) ArnT protein in 0.01% DM.

The CD spectrum of purified cysteine-free 2A6S ArnT protein was virtually identical to that of WT ArnT (Figure 4), suggesting that this cysteine-free protein retains its WT-like global folding pattern and is consistent with its ability to retain function *in vivo*. Analysis of the CD data shows that the 2A6S cysteine-free and WT ArnT proteins are composed of approximately 70% and 67% α-helical secondary structure, respectively. The PEGylation experiment was also carried out on the 2A6S protein (Figure 2B) and showed no difference between the samples in the presence and absence of mPEG-mal, consistent with a lack of cysteines,

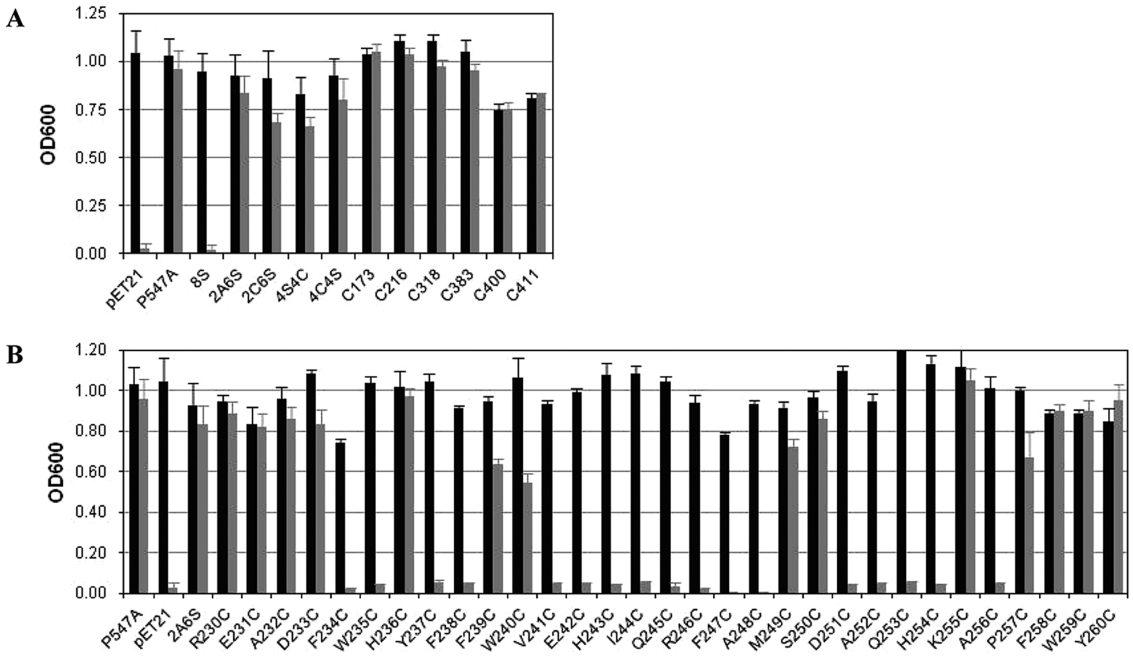

FIGURE 5: *In vivo* growth results for ArnT (A) cysteine-free constructs and single native cysteines and (B) mutations within a continuous span of more than 30 sites located in a proposed periplasmic loop. Black and gray bars represent cell growth in the absence and presence of polymyxin, respectively. Normal growth in the presence of polymyxin indicates that the mutant ArnT proteins are functional *in vivo*. Q253C has an OD_{600} in the absence of antibiotic of 1.23.

though the silver staining revealed the protein to be somewhat less pure than the WT protein.

Single Cysteine Mutant Analysis. Next, we assayed the ability of 31 single-cysteine proteins created in the functional 2A6S cysteine-free background of ArnT characterized above to complement the chromosomal ArnT knockout using an *in vivo* growth assay (Figure 5). Based on the topology model, single point mutations within a putative periplasmic loop (230−260) were assayed for *in vivo* functionality, along with single cysteine mutants retaining one of the eight native cysteines and two mixed constructs containing the first or second set of four native cysteines (4C4S and 4S4C, respectively).

Positive and negative controls are shown in both panels A and B of Figure 5 as WT ArnT (P547A) and empty vector (pET21), respectively. The three cysteine-free protein constructs (8S, 2C6S, and 2A6S) described above are shown again in graph form in Figure 5A. The 8S protein was unable to sustain cell growth in the presence of polymyxin, whereas the 2C6S and 2A6S constructs were able to fully complement the chromosomal knockout. Additionally, the first four (4S4C) and final four (4C4S) cysteines were substituted with serine and showed nearly full complementation in the growth assays. The native cysteines were reintroduced individually into the 2A6S cysteine-free background, and all were fully able to sustain cell growth in the *in vivo* assay; C148 and C149 were grouped together and are represented as 2C6S.

The majority of the substitutions in a proposed interhelical loop region (230−260) in ArnT surprisingly resulted in significant decreases in growth in the presence of polymyxin (Figure 5B). Specifically, the stretch of amino acids from 234 to 256 in ArnT, with the exception of six sites, is clearly important for function, structure, or both. In contrast, the residues located near the ends of the putative loop (i.e., 230−233 and 257−260) were able to complement the knockout following mutation to cysteine.

In order to determine if the mutations that were unable to sustain cellular growth in the presence of polymyxin were

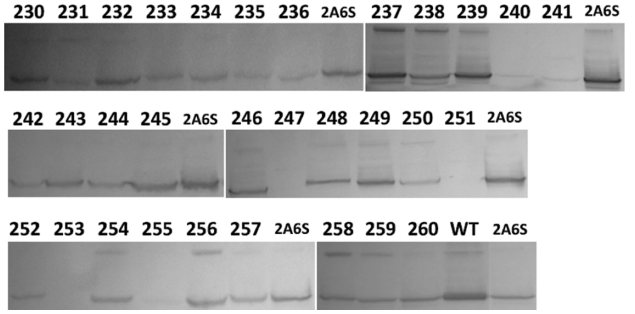

FIGURE 6: Six Western blots, each with the same 2A6S control included, are shown as one of the sets used for analysis of ArnT expression. Bands were quantified from two or three separate purifications and plotted in Figure 7.

responsible for misfolding of the protein or for direct disruption of protein function within the membrane, each mutant protein from 230 to 260 was expressed, and the amount of total protein in the membrane-solubilized fraction was determined and compared to the total amount of ArnT present in the membrane-solubilized fraction as quantitated by Western blot analysis (Figure 6).

Results of the growth assay in the presence of polymyxin are replotted next to the level of ArnT contained within the membrane fraction (as a percentage of 2A6S protein) in Figure 7. Growth assay results of each mutant protein as compared to 2A6S fall into two relatively well defined categories: 17 mutant proteins are unable to sustain growth in the presence of antibiotic and show growth of 6% or less than that of 2A6S (blue highlights, Figure 7), while all but three (F239C, W240C, P257C) of the remaining 14 mutants show growth of 85% or higher than 2A6S.

Evaluation of protein expression levels indicate that 24 mutant proteins are present within the membrane fraction at a level greater than 20% of 2A6S, four proteins are present at less than

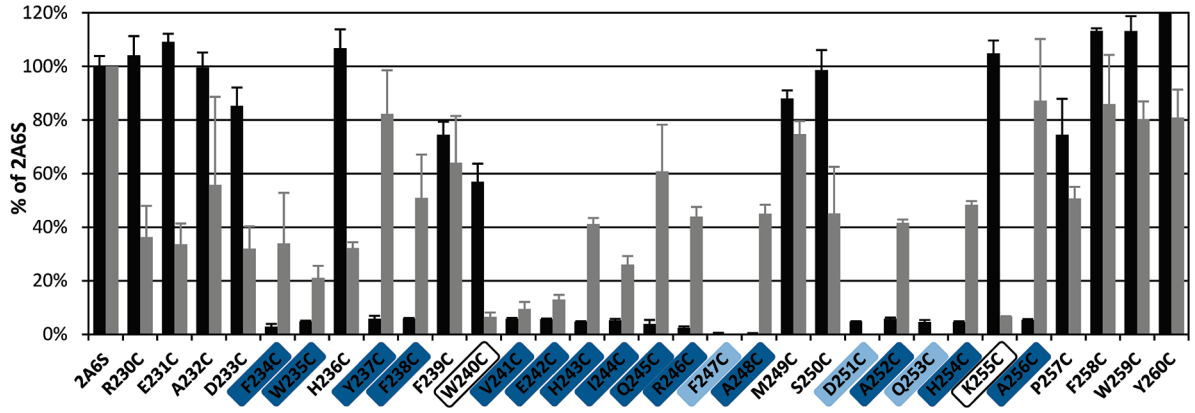

FIGURE 7: Growth and expression results plotted as a percentage of 2A6S (cysteine-free) ArnT. The growth assay results (black bars) are presented as the ratio of OD_{600} values in Figure 5 in the presence and absence of polymyxin and scaled to the 2A6S result. The amount of ArnT in the membrane fraction as a percent of the total protein in the membrane fraction (gray bars), as measured individually for each mutation, is also presented as a fraction of the 2A6S results. Unmarked mutation sites represent substitutions that sustain cell growth in the *in vivo* assay and circled sites indicate those substitutions that sustain cell growth in the presence of polymyxin despite very low expression levels (< 20%). Blue-colored sites represent those substitutions that do not sustain cell growth in the presence of polymyxin with light blue indicating no protein expression to the membrane. Total protein for 2A6S is 73 mg/2 L of cells. Total protein for the WT expression assay is 81 mg/2 L of cells, and WT ArnT expression in the membrane fraction is 0.14%.

20%, and three mutant proteins (F247C, D251C, Q253C) are undetectable in the membrane fraction. Upon comparison between the two methods of analysis (Figure 7), there are four possible categories of results: positive growth assay results and good expression (> 20%) levels of protein within the membrane fraction (unmarked), positive growth assay results and low levels of protein within the membrane fraction (circled), negative growth assay results with either low levels (blue highlights) or no protein (light blue highlights) within the membrane fraction, and negative growth assay results but with > 20% of 2A6S present within the membrane fraction (blue highlights).

Twelve mutant proteins, mainly located on the ends of the overall stretch of sites studied (230−233, 236, 239, 249, 250, 257−260), are unaffected by the cysteine substitution as indicated by complementation in the *in vivo* growth assay as well as being properly expressed into the membrane fraction. Interestingly, two mutants studied (240 and 255) that are able to sustain growth in the *in vivo* assay show very low levels of protein expression within the membrane (7%), indicating that even small amounts of these two mutant proteins are able to confer protection on the cell to polymyxin.

Of the 17 sites that showed severely diminished growth in the *in vivo* assay (blue highlights, Figure 7), 12 of the mutant proteins are expressed and present within the membrane fraction (234, 235, 237, 238, 243−246, 248, 252, 254 and 256), indicating that these point mutations likely disrupt the functional role of ArnT rather than affecting protein folding and insertion into the membrane. In fact, CD analysis of purified I244C supports this idea by showing that the protein purified from the membrane fraction is approximately 70% helical (Figure 4). Two of the remaining five of this set of mutant proteins (241 and 242) are found only at very low levels within the membrane and may be unable to function because of the small amounts of protein available. However, it should be noted that the two proteins mentioned above (240 and 255) were able to complement the knockout in the growth assay at even lower levels of protein within the membrane, so it is reasonable to group the mutations at 241 and 242 (which have protein levels of 9% and 13%, respectively, slightly higher than the 7% measured for the functional proteins 240 and 255) with the 12 outlined above that are expressed to the membrane but disrupt their ability to complement the chromosomal knockout. The three remaining mutants in this category (247, 251, and 253) show no expression within the membrane, clearly indicating that these point mutations severely disrupt protein folding or membrane insertion of ArnT. In all, we have identified for the first time a large stretch of key sites within ArnT (234−256), where 14 sites directly disrupt the function of this protein *in vivo* and 3 sites disrupt protein folding or membrane insertion when substituted with a cysteine residue.

DISCUSSION

We have utilized mPEG-mal labeling in these studies to demonstrate that ArnT derived from *S. typhimurium* does not contain disulfide bonds and that all eight native cysteines are freely reactive. This was somewhat surprising given the large number of cysteines present; however, the cytoplasm is a reducing environment, so it would not be unexpected that any cytoplasmic cysteines would be reduced. In addition, the putative topology model of ArnT suggests that several cysteines may be located within transmembrane helical segments (Figure 1), and it is unusual for disulfides to form between membrane helices. We also observed that the majority of the protein fraction was labeled with six, seven, or eight mPEG-mal moieties. In addition, none of the protein was left unmodified, indicating reasonable accessibility of each of the cysteine locations to this fairly large modifying reagent, even to the presumably buried, hydrophobic helical sites.

The absence of disulfide bonds in ArnT is further supported by the fact that the protein tolerated the substitution of all eight native cysteine residues (i.e., 2A6S) and produced a folded and functional protein. Although the 3-D structure of ArnT is not yet known, our CD and growth assay data show that none of the native cysteines are required for structural integrity or *in vivo* complementation. While the removal of all eight cysteines (2A6S) or the partial substitution of the native cysteines (2C6S) generated proteins able to complement the chromosomal knockout, the substitution of all eight cysteines with serines (8S) resulted in its inability to sustain cell growth in the presence of polymyxin. Serine is typically a suitable isosteric substitute for cysteine in

protein mutagenesis, yet this change at C148 and C149 in the 6S ArnT makes the entire protein inactive *in vivo*, while alanine mutations at these sites (2A6S) retain sufficient activity to complement the chromosomal knockout of ArnT. This suggests that proper folding of ArnT may require a hydrophobic residue such as alanine or cysteine at these positions (*23*), yet the partially native protein 4S4C remained functional *in vivo* with serines at the C148/C149 positions. Our previous experience with visual rod arrestin also required the use of a combination of alanine and serine substitutions to obtain an intact cysteine-free protein (*24*).

Next we identified a large stretch of amino acids between 234 and 256 that are required for proper function of ArnT, as assumed through complementation of the chromosomal knockout of ArnT as assessed in the *in vivo* growth assay, indicating that the proposed loop comprised of sites 229−256 is likely critical to either lipid A or the undecaprenyl phosphate-L-Ara4N recognition and binding and/or to the transfer of the L-Ara4N onto the lipid A moiety. The topology model suggests that these sites form an interhelical loop; thus we speculate that this region may be involved in recognizing and/or binding one or both of the lipid substrates after being flipped to the periplasmic leaflet of the inner membrane. This region contains nearly half polar or charged amino acids, which would be consistent with sites in this region being involved in the recognition of the lipid A phosphate groups and transfer of L-Ara4N. Of those mutants that retained the ability to confer resistance to polymyxin, two were particularly interesting; the W240C and K255C proteins were expressed at very low levels of protein within the membrane. It is possible that the mutation at these sites affects the efficiency of protein folding and/or membrane insertion, which lowers the amount of protein present in the membrane fraction, yet once integrated into the membrane the protein is still able to complement the knockout. Conversely, two other mutations (241 and 242) had low, but nonzero, levels of protein expression (9−13%) yet showed negative growth assay results. It is possible that these mutations also affect the efficiency of protein folding and/or membrane insertion, lowering the amount of protein present in the membrane fraction, but that once integrated still negatively affect protein function by interfering with or preventing substrate binding or transfer.

The above examples of small amounts of protein present in the membrane fraction highlight the fact that very low levels of functional ArnT are necessary for cellular protection against polymyxin-induced killing. It is remarkable that even at $< 0.1\%$ of the total membrane protein, functional ArnT proteins can modify sufficient lipid A to complement the chromosomal knockout by completely protecting the cell from the levels of polymyxin used in our assay.

In our survey of 31 consecutive sites in this protein we have discovered a number of critical side chains within ArnT particularly clustered between residues 234 and 256. Our results indicating that the ability of sites 257−260, all of which are aromatic in the native protein, to complement the chromosomal knockout in the growth assay upon substitution to cysteine is consistent with a model in which these sites are located within a membrane-spanning helix and not within a functionally critical soluble loop. It is tempting to relocate sites 230−233 on the opposite end of the region studied for similar reasons, but three of the four are highly polar and thus are not likely located within a hydrophobic membrane helix.

In summary, we have established here that all eight of the native cysteines in *S. typhimurium* ArnT are in the reduced form and accessible to labeling by mPEG-mal and have created a cysteine-free protein that is both structurally and functionally intact. While alanine substitution has proven useful in the early stages of protein function research, cysteine substitutions provide the opportunity for attachment of a molecular probe in future studies. Using this approach, we have identified for the first time 14 critical residues within a consecutive 31-residue span that are essential for function of ArnT and 3 additional residues that completely disrupt protein folding or insertion into the bacterial inner membrane. Our ability to generate a cysteine-free construct of ArnT allowed us to conduct cysteine-scanning mutagenesis analysis of protein expression and function and sets the stage for additional studies of the structure and function of this protein using biochemical and biophysical approaches based on site-directed cysteine labeling.

ACKNOWLEDGMENT

We thank Megan Morrell for laboratory assistance and Dr. Jimmy Feix for critical reading of the manuscript.

REFERENCES

1. Bretscher, L. E., Morrell, M. T., Funk, A. L., and Klug, C. S. (2006) Purification and characterization of the L-Ara4N transferase protein ArnT from *Salmonella typhimurium*. *Protein Expression Purif. 46*, 33–39.
2. Gunn, J. S., Lim, K. B., Krueger, J., Kim, K., Guo, L., Hackett, M., and Miller, S. I. (1998) PmrA-PmrB-regulated genes necessary for 4-aminoarabinose lipid A modification and polymyxin resistance. *Mol. Microbiol. 27*, 1171–1182.
3. Trent, M. S., Ribeiro, A. A., Lin, S., Cotter, R. J., and Raetz, C. R. (2001) An inner membrane enzyme in *Salmonella* and *Escherichia coli* that transfers 4-amino-4-deoxy-L-arabinose to lipid A: induction on polymyxin-resistant mutants and role of a novel lipid-linked donor. *J. Biol. Chem. 276*, 43122–43131.
4. Raetz, C. R., Reynolds, C. M., Trent, M. S., and Bishop, R. E. (2007) Lipid A modification systems in Gram-negative bacteria. *Annu. Rev. Biochem. 76*, 295–329.
5. Kahsay, R. Y., Gao, G., and Liao, L. (2005) An improved hidden Markov model for transmembrane protein detection and topology prediction and its applications to complete genomes. *Bioinformatics 21*, 1853–1858.
6. Kyte, J., and Doolittle, R. F. (1982) A simple method for displaying the hydropathic character of a protein. *J. Mol. Biol. 157*, 105–132.
7. Cserzo, M., Eisenhaber, F., Eisenhaber, B., and Simon, I. (2002) On filtering false positive transmembrane protein predictions. *Protein Eng. 15*, 745–752.
8. Hirokawa, T., Boon-Chieng, S., and Mitaku, S. (1998) SOSUI: classification and secondary structure prediction system for membrane proteins. *Bioinformatics 14*, 378–379.
9. Bretscher, L. E., Morrell, M. T., Funk, A. L., and Klug, C. S. (2006) Purification and characterization of the L-Ara4N transferase protein ArnT from *Salmonella typhimurium*. *Protein Expression Purif. 46*, 33–39.
10. Whitmore, L., and Wallace, B. A. (2004) DICHROWEB, an online server for protein secondary structure analyses from circular dichroism spectroscopic data. *Nucleic Acids Res. 32*, W668–W673.
11. Provencher, S. W., and Glockner, J. (1981) Estimation of globular protein secondary structure from circular dichroism. *Biochemistry 20*, 33–37.
12. van Stokkum, I. H., Spoelder, H. J., Bloemendal, M., van Grondelle, R., and Groen, F. C. (1990) Estimation of protein secondary structure and error analysis from circular dichroism spectra. *Anal. Biochem. 191*, 110–118.
13. Andrade, M. A., Chacon, P., Merelo, J. J., and Moran, F. (1993) Evaluation of secondary structure of proteins from UV circular dichroism using an unsupervised learning neural network. *Protein Eng. 6*, 383–390.
14. Kahsay, R. Y., Gao, G., and Liao, L. (2005) An improved hidden Markov model for transmembrane protein detection and topology prediction and its applications to complete genomes. *Bioinformatics 21*, 1853–1858.
15. Murakami, S., Nakashima, R., Yamashita, E., and Yamaguchi, A. (2002) Crystal structure of bacterial multidrug efflux transporter AcrB. *Nature 419*, 587–593.

16. Ward, A., Reyes, C. L., Yu, J., Roth, C. B., and Chang, G. (2007) Flexibility in the ABC transporter MsbA: alternating access with a twist. *Proc. Natl. Acad. Sci. U.S.A. 104*, 19005–19010.
17. Kast, C., Canfield, V., Levenson, R., and Gros, P. (1996) Transmembrane organization of mouse P-glycoprotein determined by epitope insertion and immunofluorescence. *J. Biol. Chem. 271*, 9240–9248.
18. Cotten, J. F., and Welsh, M. J. (1997) Covalent modification of the regulatory domain irreversibly stimulates cystic fibrosis transmembrane conductance regulator. *J. Biol. Chem. 272*, 25617–25622.
19. Palczewski, K., Kumasaka, T., Hori, T., Behnke, C. A., Motoshima, H., Fox, B. A., Trong, I. L., Teller, D. C., Okada, T., Stenkamp, R. E., Yamamoto, M., and Miyano, M. (2000) Crystal structure of rhodopsin: a G protein-coupled receptor. *Science 289*, 739–745.
20. Dawson, R. J., and Locher, K. P. (2006) Structure of a bacterial multidrug ABC transporter. *Nature 443*, 180–185.
21. Lu, J., and Deutsch, C. (2001) Pegylation: a method for assessing topological accessibilities in Kv1.3. *Biochemistry 40*, 13288–13301.
22. Guo, Z. Y., Chang, C. C. Y., Lu, X., Chen, J., Li, B. L., and Chang, T. Y. (2005) The disulfide linkage and the free sulfhydryl accessibility of acyl-coenzyme A:cholesterol acyltransferase 1 as studied by using $mPEG_{5000\text{-}maleimide}$. *Biochemistry 44*, 6537–6546.
23. Nagano, N., Ota, M., and Nishikawa, K. (1999) Strong hydrophobic nature of cysteine residues in proteins. *FEBS Lett. 458*, 69–71.
24. Hanson, S. M., Francis, D. J., Vishnivetskiy, S. A., Kolobova, E. A., Hubbell, W. L., Klug, C. S., and Gurevich, V. V. (2006) Differential interaction of spin-labeled arrestin with inactive and active phosphorhodopsin. *Proc. Natl. Acad. Sci. U.S.A. 103*, 4900–4905.